Experimental Study of Hollow Anode Position Effect on Multistage Cusped Field Thruster

IEPC-2015-407／ISTS-2015-b-407

Presented at Joint Conference of 30th International Symposium on Space Technology and Science
34th International Electric Propulsion Conference and 6th Nano-satellite Symposium,
Hyogo-Kobe, Japan
July 4 – 10, 2015

Chengyu Ma[1], Hui Liu[2], Daren Yu[3], Guoshun Sun[4], Pengbo Chen[5] and Yinjian Zhao[6]
Harbin Institute of Technology, Harbin, Heilongjiang Province, 150001, China

Abstract: **The performance characteristics of cusped field thruster are strongly associated with the anode process. In order to enhance the working gas ionization rate and diffuse anode centralized heat, a magnetic conductive hollow anode was designed. Three different anode positions were studied, where the anode surface was -8, 0 and 8 mm to the first magnet surface. The magnetic field was simulated by FEMM and the performance was tested in a vacuum system. By providing and analyzing experimental data of anode current and oscillation, thrust, anode efficiency and specific impulse, certain patterns can be found that how does the ionization rate is influenced by different anode positions. Possible explanations for increased ionization rate are given. More magnetic cusps would enhance electrons' drifting time, and a centralized electron distribution at anode surface would increase the collision probability between electrons and neutral gas.**

Nomenclature

CFT	= *Cusped Field Thruster*
AP	= *Anode position*
ISP	= *Specific impulse*
MFS	= *Magnetic Field Strength*
MC	= *Magnetic Cusp*
HA	= *Hollow Anode*
FR	= *Flow Rate*

I......Introduction

Multistage cusped field thruster is an emerging hall effect thruster recently. Have been developed by German's HEMPT[1], MIT's DCFT[2], Stanford University's CCFT[3] and many other institutes, this thruster concept mainly consists of four parts, which are magnet stages, cathode, discharging ceramic channel and anode with gas inlet. The magnet stages are located around the ceramic discharge channel, which are put in opposite poles for adjacent ones. These magnets can generate cusped magnetic field as shown in Figure.1. Electrons are released from cathode and moving towards anode direction powered by the electric field force. During the movement, electrons follow and do

[1] Student, Department of Energy Science and Engineering, Harbin Institute of Technology, machengyu19930408@gmail.com
[2] Lecturer, Department of Energy Science and Engineering, Harbin Institute of Technology, thruster@126.com
[3] Professor, Department of Energy Science and Engineering, Harbin Institute of Technology, thruster@126.com
[4] Student, Department of Energy Science and Engineering, Harbin Institute of Technology, 1437140573@qq.com
[5] Student, Department of Energy Science and Engineering, Harbin Institute of Technology, 1151786040@qq.com
[6] Student, Department of Energy Science and Engineering, Harbin Institute of Technology, 1634466984@qq.com

E x B drift around the magnetic induction lines generated by magnet stages due to hall effect. Accelerated by electric field, high energy electrons can ionize the working medium injected from anode gas inlet. With normal working medium of xenon, the ionization procedure will consume one electron and generate two electrons for each xenon atom. This progress will maintain the ionization for more xenon atoms. When the electrons move into a MC, the magnetic mirror effect will confine the electrons move between two adjacent cusps. This effect can increase the transfer time of electrons in discharge channel, which can result in a higher ionization rate. Besides, due to the higher MFS distributed along the channel surface, this magnetic mirror effect will reduce the collision effect of ions and electrons to channel wall, which can increase the lifetime of the thruster. Due to this thruster's features of long lifetime, high efficiency, small volume and wide thrust range[4], it has potential application interests in small satellite propulsion system.

A high efficiency CFT that developed by German has 3 stages[5]. However, the effect of the position of the anode has not been clearly demonstrated yet. With different anode positions, the magnetic field cusp number along the channel varies. During the movement of electrons and ions along the channel, different cusp number can result in difference in ionization rate, ionization position and acceleration performance. In order to find these effects of different anode positions, a set of experiments were carried out and analyzed.

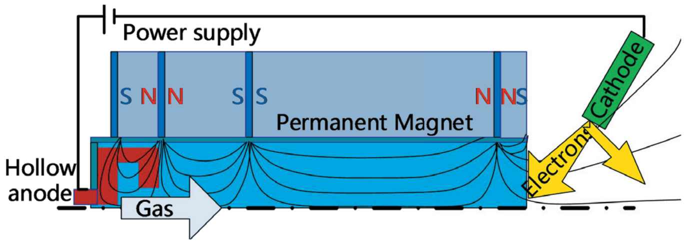

Figure. 1 Cusped field thruster concept.

II......Thruster design and Magnetic field simulation

A. Thruster design

In order to change the anode position in the thruster channel, a thruster designed by Harbin Institute of Technology that has a length variable multistage modular ceramic channel wall has been used, as illustrated in Figure. 2. When the position of the hollow anode need to be changed, the number of the ceramic channel wall modules can be combined, increased or decreased. The ceramic channel wall modules have an inner diameter of 40mm and wall thickness of 2mm, with the height of 8mm or 10mm. The magnet stages are designed as hollow cylinders, with an inner diameter of 64mm and outer diameter of 88mm. The heights of each magnet stages are 8mm, 16mm, 48mm and 4mm, from the first anode side to the last external stage. Has been proved in previous experiments, this magnet stages length distribution is designed to maintain the thruster in a good performance[6]. Between any two adjacent magnet stages, there lies the magnetic field conductive rings, which are used to strengthen the MC field[7].

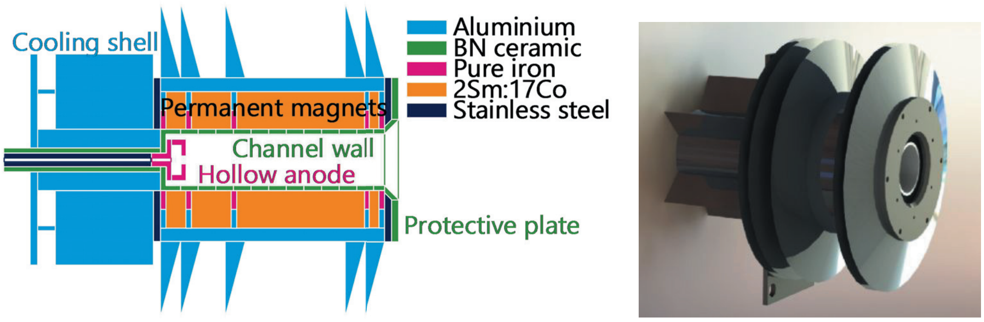

Figure. 2 Experimental multistage cusped magnetic field thruster.

In order to reduce the heat centralization in anode and to increase the ionization rate, the anode is designed as a hollow cylinder with a hole at the bottom surface. The right surface of the HA is covered by a ceramic shell, which is to prevent the electrons' loss by colliding with that bottom surface. The anode is made of pure iron.

B. Magnetic field design

The overall magnetic field distribution along the channel is shown as Figure. 3. There are 4 MCs along the channel. During the experiments, this magnet stages distribution remains unchanged.

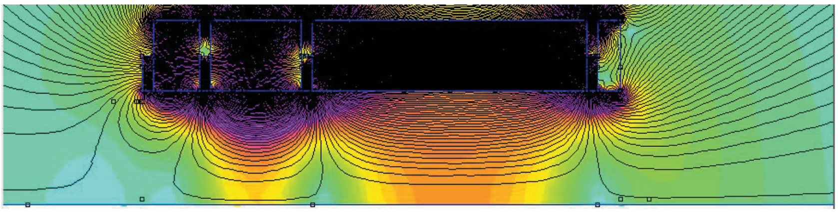

Figure.3 Overall magnetic field distribution along the channel.

The magnetic field simulation results of different anode positions are shown as Figure. 4. In the legend of this figure, purple color represents 0.285-0.3T, and light blue represents 0 to 0.015T. Most parts of the magnetic field distribution along the channel is similar among different anode positions. In order to focus on the difference in these magnetic fields, only the area of first, second, and partial third magnet stage are displayed. For the purpose of showing the difference in the HA chamber clearly, the color bar legend in these simulations has a higher sensitivity compared to that in Figure.3. Purple color represents 0.00019-0.0002T, with light blue representing 0 to 0.00001T. As to clearly demonstrate the change of magnetic field, there are 12 different positions of anode have been simulated in gap of 2mm, which are 10mm, 8mm, 6mm, 4mm, 2mm, 0mm when the anode top surface is ahead of the magnet bottom surface, and 2mm, 4mm, 6mm, 8mm, 10mm and 12mm for the distance in the reverse direction.

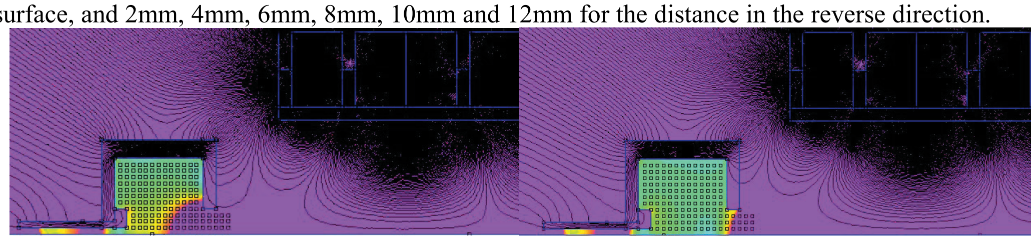

10mm 8mm

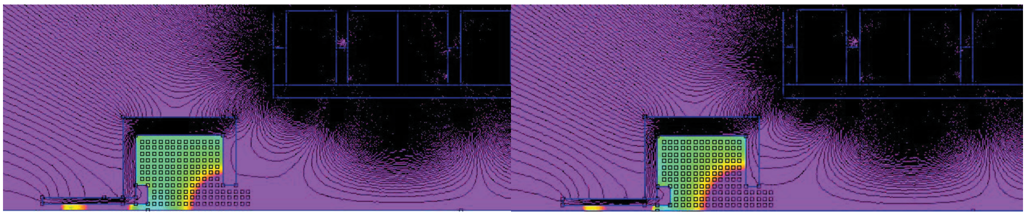

6mm 4mm

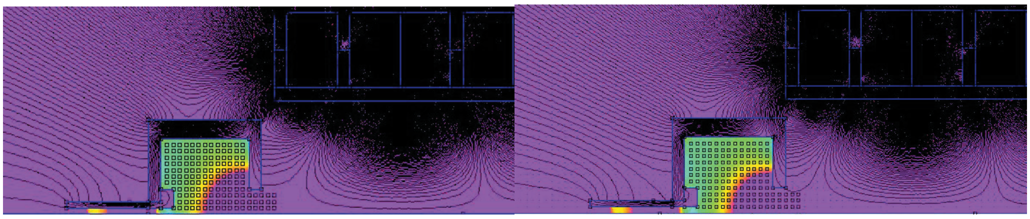

2mm 0mm

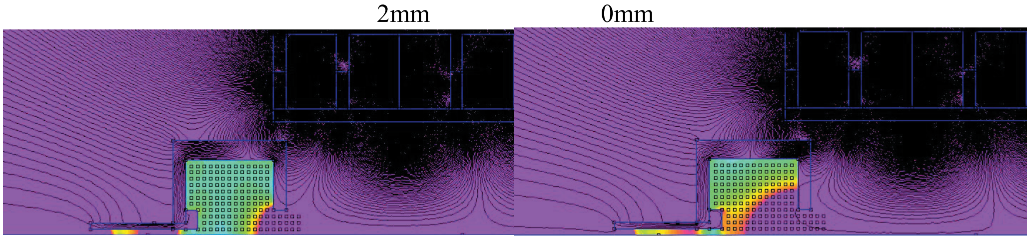

-2mm -4mm

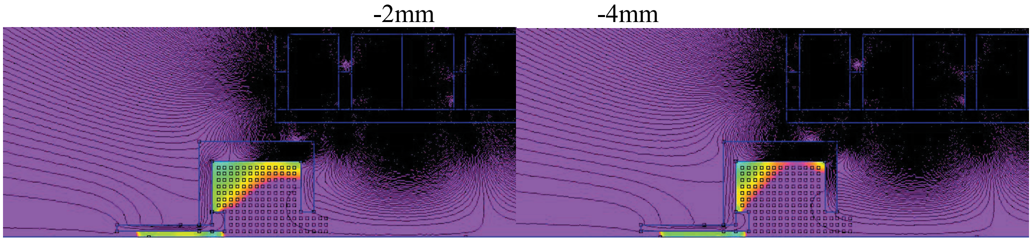

-6mm -8mm

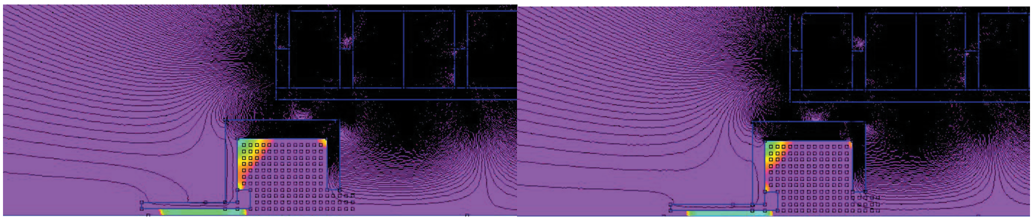

-10mm -12mm

Figure. 4 Magnetic field simulations near anode of different anode positions.

From the figures above, it can be found that in the first 2 figures, there are 3 magnetic field cusps generated in the channel, when the position of anode top surface is 10mm and 8mm ahead of magnet bottom surface. Accounting for the top cusp that is not shown in the figures, there are 4 MCs for xenon to ionization and acceleration along the channel. In comparison, the magnetic fields in figure 3 to 7 have 3 MCs along the channel, while there are only 2 cusps in figure 8 to 12. This is because the magnetic conductive shell will absorb and influence the original magnetic field. When the anode is put backwards into the channel, more of the forward cusps are absorbed by the anode.

Due to the absorption of effective magnetic field conductive shell, the MFS in this empty space are relatively very low. There is a high MFS gratitude near anode top surface center. It can also be found that, the magnetic induction lines within this space are distributed in radiation directions, from the top surface center to anode inner round side wall. From previous experimental study, the main ionization area is around the center axis of the channel, where most electrons are gathering. Due to the electrons' movement will follow the magnetic induction lines, they will distributed more evenly in this chamber. As xenon is injected into the chamber from the bottom pipeline, the ionization rate will be higher in this chamber theoretically. In order to suit small satellite applications with limited power supply, this design is intended to have a good performance in low voltage below 200V.

Another fact that can be observed is the change trend of the MFS within the HA chamber. With the placement of HA going backwards, the MFS in the chamber increases generally. This is because the anode is entering a section with stronger environment magnetic field, and the pure iron shell's absorption of magnetic induction lines tend to be saturated. But there are 2 special figures do not this change pattern, which are when the anode top surface is 8mm ahead of the magnet bottom surface, and when it is 2mm behind. In these 2 cases, the MFS in the chamber reduces to the lowest level compared to their adjacent figures. However, due to they all have very weak magnetic field compared to the outside area, the effect of different chamber inside MFS can be ignored.

III......Experimental facilities

The experiments were carried out in the vacuum chamber at Harbin Institute of Technology. Because the environment air pressure has a great influence on thruster's operation, both in ignition voltage and common discharge current during operation. Hence, in the vacuum chamber, the air pressure is reduced and kept at 2.7*10^-3Pa, which can create a suitable environment similar to space for thruster to operate safely. The power supply can provide up to 500V anode voltage. The anode flow rate can be adjusted from 0sccm to 50sccm. The working medium gas was xenon. The cathode was chosen as the hollow cathode, which can heat xenon into ionization state to generate electrons. The flow rate of cathode xenon was kept at 3sccm. Due to the position and pointing angle of cathode can influence the performance which can be observed from previous experiments, during the experiments, the position of cathode exit is maintained at the outside of the channel exit by 50mm high and 50mm back from the circular exit center. The pointing angle of the cathode is 45 degree with the horizontal axis. The keeper voltage was kept at 21V. Other parameters were not changed during the experiments.

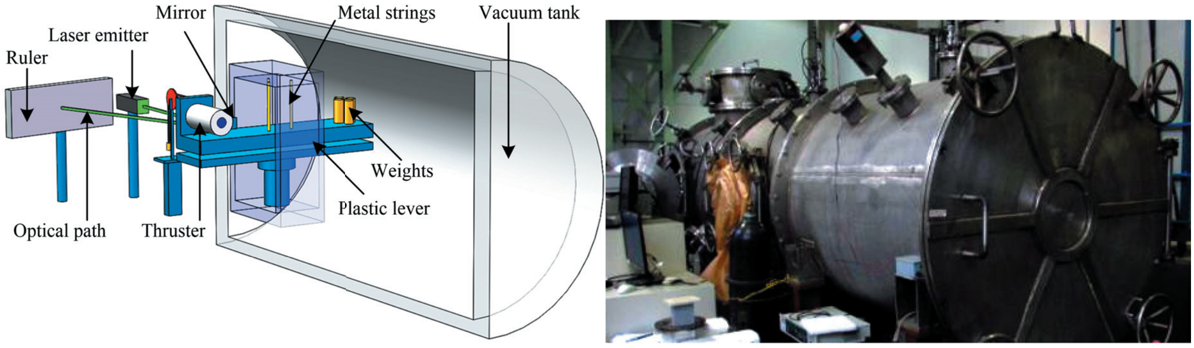

Figure. 5 Thruster experimental system.

IV......Experimental results and analysis

In order to analysis the effect of cusps number along the channel caused by different anode position, 3 different anode positions are analyzed in these experiments. The first position is when the top surface of HA at 8mm ahead of the magnet bottom. With the forward gap of 8mm each time, 2 more positions are placed at the distance of 0mm and 8mm back.

By measuring the the laser point deflection ratio and anode current in different anode FR and voltage, the performance parameters such as efficiency and ISP can be calculated by the following formulas.

Anode efficiency η_a :

$$\eta_a = \frac{T^2}{2 \times m_a U I} \tag{1}$$

where T is the thrust, U is the anode voltage, I is the anode current and m_a is the mass flow rate of working medium.

Due to the experimental flow controller was set as volume flow unit $sccm$, hence anode mass flow rate m_a:

$$m_a = \frac{l_a}{60 \times 10^6} \cdot \rho_{Xe} \tag{2}$$

where ρ_{Xe} is the density of xenon in standard atmosphere.

Anode specific impulse I_{sp} is defined as:

$$I_{sp} = \frac{T}{\dot{m}_a g} \tag{3}$$

where g is the standard of gravity acceleration.

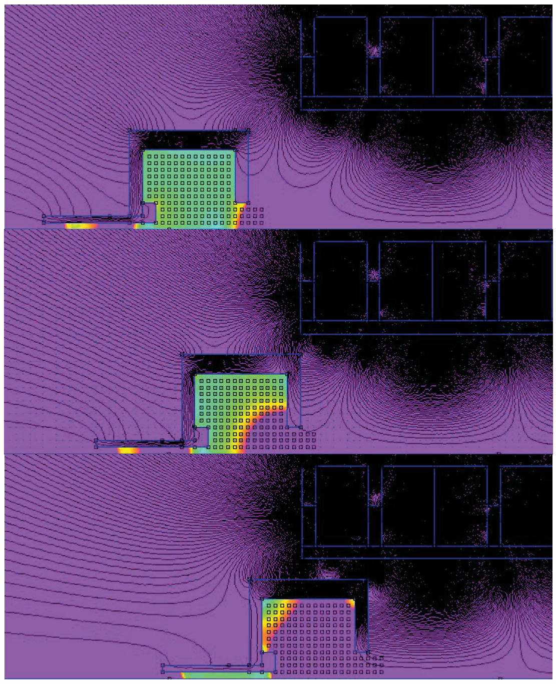

Figure. 6 Magnetic field distribution in 3 anode positions for experiments.

According to precious experiments[vii], the measured error is estimated as 5% of the original value for anode current and thrust, as result, it also exists in the calculated value of efficiency and ISP.

The anode current change with voltage in different FR among these 3 anode positions are shown as following in Figure.7. The representation of line colors for different anode flow rates in this figure are used throughout this paper.

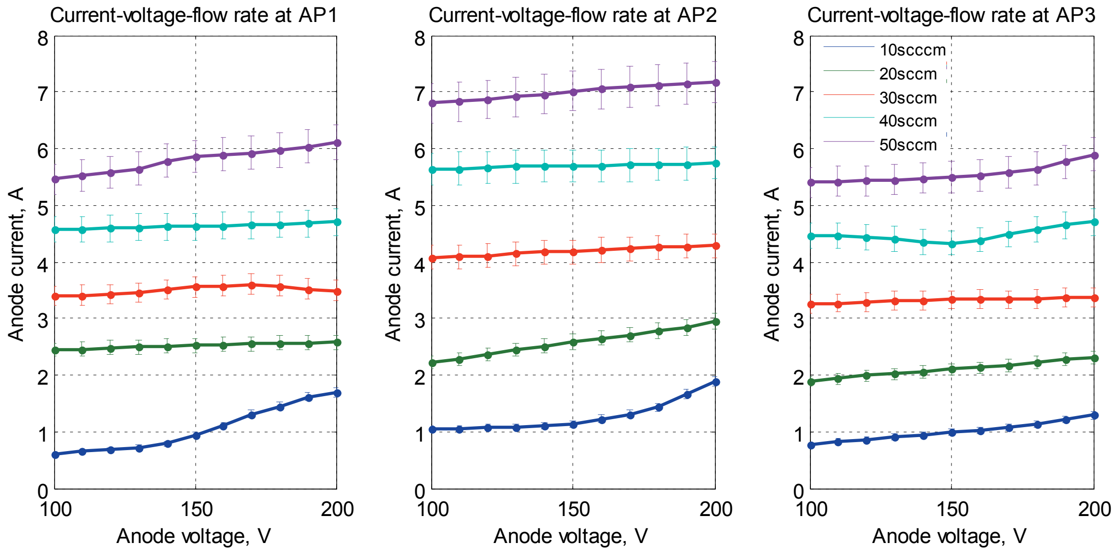

Figure.7 Anode current change with anode voltage and flow rate in different anode position.

According to the curves, generally, with the increasing anode voltage from 100V to 200V, the anode current increases as well. The current also increases with the anode FR. The maximum voltage that achieved in the experiments is 200V in 50sccm of AP2. In higher voltage, the thruster turns to operate unstably with strong anode current oscillation. In order to protect experiment facilities, higher voltage operations more than 200V were not measured and recorded. At 200V and 50sccm, the anode current in AP1 is 6.12A and input power is 1224W. In AP2 and AP3, the current are 7.17A and 5.9A, with power supply of 1434W and 1080W respectively. The current and power consumption in AP2 is the highest, while the third position is the lowest. The value difference is more effective at higher anode FR. At higher FR than 30sccm in AP2, the anode current undertook the strongest oscillation, which caused unstable operation of the thruster.

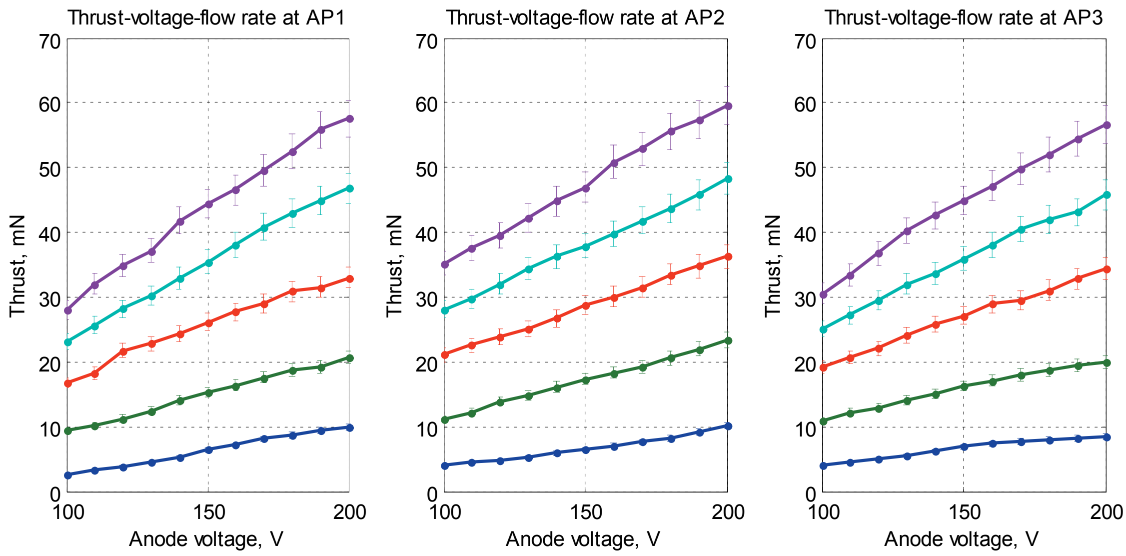

Figure.8 Thrust change with anode voltage and flow rate in different anode position.

According to the thrust change curves along with anode voltage and anode FR in different positions that shown in Figure.8 as above, the thrust increases with higher anode voltage and FR, in a relatively linear trend. For AP1, the maximum thrust of 57.52mN is achieved at 200V with anode FR of 50sccm. At the same anode voltage and FR, the highest thrust in AP2 and AP3 is 59.59mN and 56.65mN. Similar to the anode current and power comparison, the thrust in AP2 is also the highest.

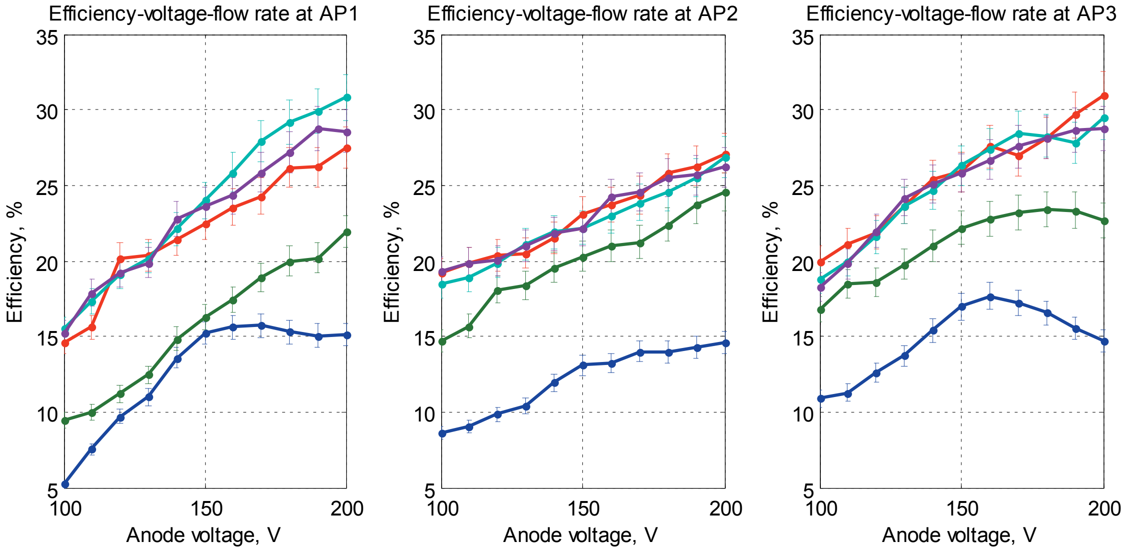

Figure.9 Efficiency change with anode voltage and flow rate in different anode position.

The Figure.9 above illustrates the calculated efficiency change patterns for different anode positions, along with anode voltage and FR. The efficiency increases firstly with anode voltage from 100V, but the increasing rate gets lower with higher voltage. Until the efficiency reaches the highest value and the efficiency starts to drop. For example, in AP3, for 10scmm curve, the maximum efficiency of 17.67% occurs in 160V. Also, in higher anode FR, the top efficiency and its corresponded voltage turns to be higher as well. Similarly, the efficiency also increases with FR from 10scmm. However, at the FR higher than 30sccm, the efficiency turns to be stable and starts to decrease.

In AP1, the highest efficiency of 30.82% occurs at 200V with 30sccm. While in the AP2 and AP3, the maximum efficiency are 27.13% and 31.01%, at 200V with same FR of 30sccm. Generally, the efficiency in AP2 is the lowest in higher FR than 30scmm. While in 10sccm and 20sccm, AP2 still have a relatively effective performance. The AP3 has the highest efficiency during the experiments.

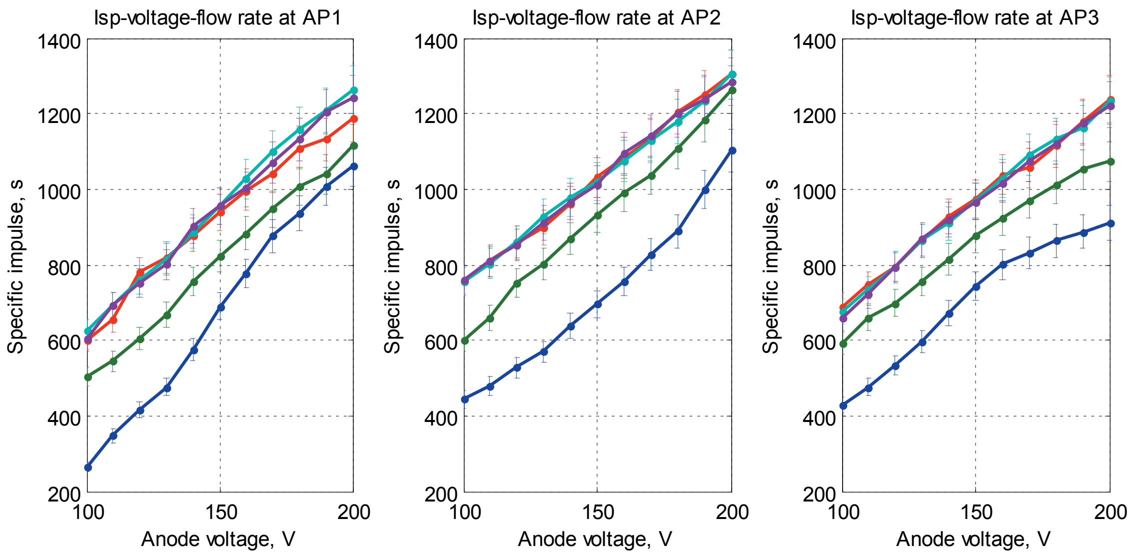

Figure.10 ISP change with anode voltage and flow rate in different anode position.

The calculated ISP in 3 anode positions along with anode voltage and FR are shown in Figure.10 above. Basically the ISP increases with the voltage from 100V to 200V. However, with the increase of anode FR, the ISP increases firstly and then turns to be stable after 30sccm. The maximum ISP in AP1 is 1241s at 200V at 40sccm, while it is 1304s and 1235s in AP2 and AP3 at the same voltage and FR. It can be observed that the AP2 has the highest ISP, then follows the AP3, while AP1 has the lowest ISP.

V......Plasma dynamic analysis

From the experimental data analyses above, it can be found that the AP1 has an average performance in anode current and thrust, while it has low performance in efficiency and ISP especially in low voltage and FR. However, the performance increasing rate is the highest along with voltage and FR. This is due to the anode current grows slowly while thrust grows rapidly, which means the AP1 has a better general performance only in high voltage and FR. This can be explained by the following reasons. From the magnetic field simulation in Figure.6, the AP1 has 4 cusps in front of the anode. These 4 cusps confine the electrons more effectively compared to the other two positions, which make it harder for low energy electrons to ionize the gas in lower voltage[8]. However, when the voltage is higher, the high energy electrons can be more relatively effectively confined in these cusps area, which is the advantage of these cusps. In addition, due to the wide diameter of the cusps near anode, which caused the distribution of electrons, the ionization rate can be lower at low gas density, while this effect turns to be better at higher FR.

In comparison, the second one has the largest anode current, thrust and ISP among these 3 anode position. Due to the fast growing anode current, its efficiency is the lowest in high anode voltage and FR. Thruster in this AP has better performance in low voltage and FR, and it is not suitable for operation in high FR more than 30sccm due to severe anode current oscillation. The anode bottom is about 2mm ahead of the top MC at the AP2. As this cusp may be one of the major cusps that constrain electrons to ionize neutral gas[9], at low voltage and FR, the electrons movement keeps stable and can be effectively received by anode chamber inside, following magnetic induction lines. However, at higher gas density and voltage, more high energy electrons are spread along magnetic induction lines with wider diameter[10]. These electrons will collide into the ceramic surface that covers the anode. Due to the electrons' accumulation in the surface, the ceramic can generate a reverse electric field that prevent further electrons collision[11]. As a result, the electrons will also statically accumulate outside the anode top surface, of which the electric field will cause unstable movement of electrons near the cusp, causing oscillation of anode current.

The AP3 has the most stable operation during the experiment. It has the lowest anode current, while it has similar thrust with AP1, which contributes to the highest general efficiency. The anode position is relatively away from cusp, which lead to less influence to the performance from electric field generated at ceramic surface.

VI......Conclusion

From the experiments it can be found that, anode position can greatly influence the thruster performance.

When the anode bottom surface is 8mm ahead of magnet stage top surface, the thruster has a better performance at higher anode voltage than 150V and higher FR than 30sccm. Considering efficiency, the AP2 has a better performance only when the anode voltage is lower than 150V or FR lower than 30sccm. The AP3 has a stable overall performance during different anode voltage and flow rate. While it has the average thrust, but it has the highest efficiency.

In order to get more information of how anode position interact with plasma dynamics, different overall magnetic field should also be studied in the future. For example, different length of the first magnet stage may have different interaction with the anode position effect, which can be valuable to further research.

Acknowledgments

This research is funded by the Foundation for Innovative Research Groups of the National Natural Science Foundation of China (Grant No. 51121004) and National Natural Science Foundation of China (Grant Nos. 51207033 and 11275055).

Experimental facilities and modular length variable multistage cusped field thruster are supported by the plasma group of advanced propulsion research institute at Harbin Institute of Technology.

References

[1] G. Kornfeld, N. Koch and H. P. Harmann, Proceedings of the 30th International Electric Propulsion Conference, Florence, Italy, 2007 (Electric Rocket Propulsion Society, Fairview Park, 2007), IEPC Paper No. 2007-110.

[2] D. G. Courtney, P. Lozanoy and M. Martinez-Sanchez, Proceedings of the 44th Joint Propulsion Conference, Hartford, CT, 2008 (American Institute of Aeronautics and Astronautics, Washington D.C., 2008), AIAA Paper No. 2008-4631.
[3] C. V. Young, A. W. Smith and M. A. Cappelli, Proceedings of the 31st International Electric Propulsion Conference, Ann Arbor, USA, 2009 (Electric Rocket Propulsion Society, Fairview Park, 2009), IEPC Paper No. 2009-166.
[4] Koch, N., et al. "Development, Qualification and Delivery Status of the HEMP-T based Ion Propulsion System for SmallGEO." Proceedings of the 32d International Electric Propulsion Conference. 2011.
[5] Koch, N., H. P. Harmann, and G. Kornfeld. "Status of the THALES High Efficiency Multi Stage Plasma Thruster Development for HEMP-T 3050 and HEMP-T 30250." Proceedings of the 30th International Electric Propulsion Conference. 2007.
[6] Liu, H., Sun, G., Zhao, Y., Chen, P., Ma, C., Wu, H., & Yu, D. (2015). Plume Control of a Cusped Field Thruster.
[7] Ma, C., Liu, H., Hu, Y., Yu, D., Chen, P., Sun, G., & Zhao, Y. (2015). Experimental study on a variable magnet length cusped field thruster. Vacuum, 115, 101-107.
[8] Zhurin, V. V., H. R. Kaufman, and R. S. Robinson. Physics of closed drift thrusters. Plasma Sources Science and Technology 8.1 (1999): R1.
[9] Daspit R M. Performance characterization and optimization of a diverging cusped field thruster with a calibrated counter-weighted millinewton thrust stand[D]. Massachusetts Institute of Technology, 2012.
[10] Courtney, D. G., Lozanoy, P., & Martinez-Sanchez, M. (2008). Continued investigation of diverging cusped field thruster. AIAA Paper, 4631, 2008.
[11] Raitses, Yevgeny, et al. "Electron-wall interaction in Hall thrustersa)." Physics of Plasmas (1994-present) 12.5 (2005): 057104.